Comments

Comments are short papers which comment on papers of other authors previously published in the **Physical Review**. *Each Comment should state clearly to which paper it refers and must be accompanied by a brief abstract. The same publication schedule as for regular articles is followed, and page proofs are sent to authors.*

Comment on "Use of Dirichlet boundary conditions for electron-atom scattering"

H. R. Sadeghpour*
Department of Physics and Astronomy, Louisiana State University, Baton Rouge, Louisiana 70803
(Received 14 November 1988)

Electron correlations in H^- are represented with a model interaction potential, $1/(r_1+r_2)$. Hyperspherical-coordinate wave functions describing strong electron correlations near the origin are matched onto dipole field quantum-defect functions far from the nucleus. The results of this calculation complement and in some respects differ from those of Altick [Phys. Rev. A **38**, 33 (1988)].

In a recent paper, Altick[1] examined the scattering of electrons from the hydrogen atom by modeling the radial-electron correlations present in H^- with an interaction potential $1/(r_1+r_2)$. Our interest in studying this potential has been motivated by (1) the fact that the Wannier threshold law for the escape of electrons from a positive ion has been shown to emerge when the electron interaction is modeled by this potential,[2] and (2) the realization that it embodies many other features of the real two-electron interaction potential $1/r_{12}$. [One such feature common to both electron-electron interactions in H^- is that their adiabatic hyperspherical potential form at large $R=(r_1^2+r_2^2)^{1/2}$ evolves to a "dipole" potential.] In this Comment we present some preliminary calculations in the same energy range treated in Ref. 1 demonstrating the validity of a combined hyperspherical and quantum-defect-type description and clarifying some points not addressed in detail in Ref. 1.

The present numerical technique combines a nonadiabatic hyperspherical calculation with multichannel quantum-defect theory[3-5] (MQDT). The coupled differential equations in the hyperspherical radius can be given in a compact form[6]

$$\left[\left[\underline{I}\frac{d}{dR}+\underline{P}(R)\right]^2+2[\underline{I}E-\underline{U}(R)]\right]\mathbf{F}(R)=\mathbf{0}\ , \qquad (1)$$

where $\underline{I}$ stands for the identity matrix. The couplings between different adiabatic channels $U_n(R)$ are represented by the antisymmetric matrix

$$P_{nn'}(R)=\langle\phi_n|(d/dR)\phi_{n'}\rangle\ ,$$

where $\{\phi_n\}$ includes the infinite set of complete orthogonal adiabatic eigenfunctions.[6] The components of the solution matrix $F_{n\beta}(R)$ in each channel are propagated outward from the origin to matching radius R_0. A fairly well-known stabilization procedure ensures linear independence of the solution vectors.[7]

The slow convergence at large R of the channel couplings, $P_{nn'}(R)\propto R^{-1}$, represents a drawback of the adiabetic hyperspherical description. Attempts at remedying the problem have included matching the hyperspherical solutions at some intermediate R to close-coupling wave functions in independent-electron coordinates.[8,9] We will demonstrate here that a combined hyperspherical and quantum-defect method can adequately describe the long-range phenomena in terms of a few parameters weakly dependent on the energy. To this end we use the fact that the adiabatic potentials tend asymptotically to dipole potentials[10] of the form $-a_n/(2R^2)$, where $a_n=3n^2$ gives the dipole moment in the nth channel. [At $R_0=14$ a.u., $U_1(R_0)$ is different from a dipole potential by less than 2%. We nevertheless caution that the formation of a dipole moment in the lowest channel is an unrealistic property of this interaction potential.] It should also be noted that we include in the potential matrix $\underline{U}(R)$ in Eq. (1) a diagonal correction term $-\frac{1}{2}(Q_{nn}(R)+\sum_{n'=1}^{N}|P_{nn'}|^2)$.[11] The corrective term is added to the diagonal potential matrix to compensate for the truncation of the adiabatic basis set. We have found that otherwise the truncated sum suffers from an incorrect convergence at large hyper-radii.

The analytical framework then connects naturally to a quantum-defect analysis,[12]

$$\sum_{\beta=1}^{N_0}F_{n\beta}(R_0)c_{\beta\nu}=f_n(R_0)U_{n\nu}\cos(\pi\mu_\nu)-g_n(R_0)U_{n\nu}\sin(\pi\mu_\nu)\ , \qquad (2)$$

where $\nu=1,\ldots,N_0$. Here $F_{n\beta}$ are the elements of the solution matrix in the open or weakly closed ^1S channels (a similar equation holds for the derivatives as well), μ_ν

are the well-known short-range quantum defects (or phase shifts $\pi\mu_\nu$) in each channel n, $U_{n\nu}$ are the orthogonal-frame transformation-matrix elements connecting the detachment channels n and the eigenchannels ν [not to be confused with the potential-matrix elements of Eq. (1)], [5,12] f_n and g_n are, respectively the energy-normalized regular- and irregular-type dipole functions[10] at the matching radius R_0, and N_0 is the number of open or weakly closed channels. A similar linear superposition in the strongly closed channels must of course decay exponentially outside this prescribed "one-dimensional box" enclosed within $R=R_0$. Short-range knowledge of the strong-electron correlations is obtained by solving Eq. (2) for $\pi\mu_\nu$ and $U_{n\nu}$. The contributions from the long-range field to the scattering process are included in the scattering matrix through the long-range phase shift $\eta(k_n,\alpha_n)=\phi(k_n,\alpha_n)-\pi/4$ pertaining to each open channel n,[13] with

$$\phi(k_n,\alpha_n)=\tan^{-1}\left[-\frac{\tan[\alpha_n\ln(k_n/2)+\chi_\alpha]}{\tanh(\pi\alpha_n/2)}\right]. \quad (3)$$

Here $\chi_\alpha=\arg[\Gamma(1-i\alpha_n)]$, $\alpha_n=(a_n-\frac{1}{4})^{1/2}$, and $\frac{1}{2}k_n^2=\varepsilon_n$ represents the incident energy relative to the nth threshold.[10] We give here only the expression for the elastic scattering cross section σ_{11} just above the lowest detachment threshold ($\varepsilon_1\sim 0$) to emphasize the presence of low-energy oscillations in σ_{11} and also the infinite number of bound levels, which are guaranteed by the dipole field alone,

$$\sigma_{11}=(2/\varepsilon_1)\sin^2(\pi\mu+\eta) \quad (4)$$

in units of πa_0^2, where a_0 is the Bohr radius.

The oscillatory logarithmic dependence of the elastic cross section on the energy is depicted graphically in Fig. 1 (inset). The smooth oscillations of the cross section just above the threshold are manifestations of the exponential convergence, as $\varepsilon^{(m)}=\varepsilon^{(0)}\exp(-2m\pi/\alpha)$, of the discrete states in the dipole field just below the threshold.[10,14,15] (Note that a generalized form of the MQDT applicable to the dipole field is needed here to arrive at this exponential form.[10]) This simple analytical argument shows that Altick's assertion that this model Hamiltonian for the negative ion supports only two bound states is incorrect. (See also the erratum in Ref. 16.) Table I gives the positions of the first three discrete levels in the $n=1$ channel. For comparison, the $1s^2$ energy is calculated three different ways. The first entry in Table I is obtained from a direct numerical integration of Eq. (1) and forcing all the components of the solution vectors to vanish on a large-R boundary (strongly closed channels). The second entry is found by following the prescription of Eq. (2) and allowing the numerically integrated solutions to match at a smaller radius $R_0=14$ onto the long-range dipole functions for the lowest channel. The third entry is an "exact" calculation obtained by diagonalizing the model two-electron Hamiltonian in a large independent-electron basis confined to a finite volume.

We also show in Fig. 1 the resonances converging to the $n=2$ and $n=3$ thresholds. A three-channel hyperspherical MQDT calculation below the $n=2$ threshold with the "box" boundary at $R_0=14$ a.u. produces the structures shown in Fig. 1. In the energy range below the $n=3$ threshold, four channels are included in the analysis and the boundary is moved out to $R_0=30$. The highest channel is treated here as strongly closed. Our results compare well with Altick's variational calculation using 55 two-electron functions to form the inner solutions which vanish on a boundary at $r=40$. (In Fig. 1 the data of Ref. 1 are multiplied by a factor of 4. This factor is associated with the spin averaging.[17]) But a minor discrepancy concerns the position of the lowest resonance in the $n=3$ channel. This resonance shows up in σ_{11} in Fig. 1 at 0.426 6 a.u. above the first-ionization threshold, the "blip" reported in Ref. 1 as the lowest res-

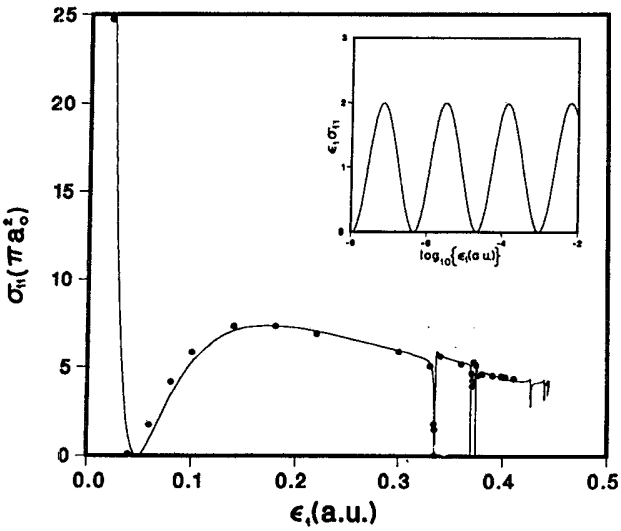

FIG. 1. The elastic cross section σ_{11} (in units of πa_0^2) as a function of the energy above the $n=1$ threshold ε_1 (a.u.). The data points, rescaled by a factor of 4, are taken from Table I of Ref. 1. The inset figure shows the same cross section, rescaled by ε_1 to compensate for the divergent amplitude of σ_{11} as $\varepsilon_1\to 0$, on a logarithmic energy scale. This demonstrates how the first zero of σ_{11} near $\varepsilon_1\sim 0$ is another manifestation of the long-range dipole field.

TABLE I. Bound-state ^1S energy levels (in a.u.) for H^- with the electron interaction modeled by the $1/(r_1+r_2)$ potential.

Designation	No. of adiabatic channels	Energy level relative to $n=1$ (a.u.)
$1s^2$	3[a]	−0.146 52
$1s^2$	3[b]	−0.146 53
$1s^2$	"Exact"[c]	−0.146 48
$1s2s$	3[b]	-2.6640×10^{-3}
$1s3s$	3[b]	-6.0325×10^{-5}

[a]Without MQDT.
[b]With MQDT.
[c]Diagonalization of the full Hamiltonian with 120 symmetrized products of 15 "closed-type" one-electron functions confined to a volume of radius $r_0=15$.

onance occurs at 0.398 0 a.u. A simple search for the adiabatic $3s^2$ discrete state finds the energy level at 0.421 5 a.u. This resonance has a width (in a.u.) of $\Gamma_1 \simeq 1.4\times10^{-3}$, as compared to $\Gamma = 1.5\times10^{-3}$ for the lowest ^1S resonance of the real H^- ion below the $H(n=3)$ threshold at 0.4310 a.u.[18,19] The second-lowest resonance below the $n=3$ threshold at 0.4398 a.u. has a width of $\Gamma_2 \simeq 6.5\times10^{-4}$. Note also in Fig. 1 that the low-energy zero of the elastic cross section near $\varepsilon_1 \sim 0.05$ a.u. is the result of the long-range phase-shift oscillations discussed above [see also Fig. 1 (inset)]. The next-highest zero would occur about 4 a.u. above the $n=1$ threshold.

In concluding we remark that the combined hyperspherical and quantum-defect treatment lends itself readily to the description of both the short- and long-range effects of the potential field in terms of a few smooth parameters regardless of inaccuracies in the short-range calculation. The behavior dictated by the long-range dipole field just below and immediately above the ionization threshold is correctly accounted for with these parameters. The low-energy oscillations of the elastic cross section and the infinite number of bound states below an ionization threshold are shown to be direct consequences of this asymptotic dipole field.

The author is indebted to Professor C. H. Greene for his invaluable suggestions during the completion of this work and for a critical reading of the manuscript. The author also benefited from fruitful discussions with Professor A. R. P. Rau and Professor P. L. Altick. This work was supported in part by the National Science Foundation Grant No. 83-51007.

*Present address: Joint Institute for Laboratory Astrophysics, University of Colorado, Boulder, CO 80309.

[1]P. L. Altick, Phys. Rev. A **38**, 33 (1988).
[2]R. Peterkop. J. Phys. B **4**, 513 (1971); **16**, 587 (1983).
[3]J. H. Macek, J. Phys. B **1**, 831 (1968); C. D. Lin, Phys. Rev. A **10**, 1986 (1974).
[4]M. J. Seaton, Proc. Phys. Soc. London **88**, 801 (1966); Rep. Prog. Phys. **46**, 167 (1983).
[5]U. Fano, Phys. Rev. A **2**, 353 (1970).
[6]H. Klar, Phys. Rev. A **15**, 1452 (1977).
[7]R. G. Gordon, J. Chem. Phys. **51**, 14 (1969).
[8]B. L. Christensen-Dalsgaard, Phys. Rev. A **29**, 2242 (1984).
[9]J. Macek, Phys. Rev. A **31**, 2162 (1985).
[10]C. Greene, U. Fano, and G. Strinati, Phys. Rev. A **19**, 1485 (1979).
[11]The matrix $Q_{nn'}(R)=\langle\phi_n|(d^2/dR^2)\phi_{n'}\rangle=\sum_m P_{nm}(R)R_{mn'}(R)+(d/dR)P_{nn'}(R)$ originally appears in the coupled radial Schrödinger equations [see Eq. (2) of Ref. 6]. Its equivalent form as the sum over the infinite adiabatic basis set $\{\phi_m\}$ is used in arriving at the compact form of the coupled differential equations, Eq. (1).
[12]C. H. Greene and Ch. Jungen, Adv. At. Mol. Phys. **21**, 51 (1985).
[13]Note that Table I of Ref. 10 contains a misprint. The correct branch of $\phi(k,\alpha)$ should instead be the same as $-[\alpha\ln(k/2)+\chi_\alpha]$.
[14]C. D. Lin, Phys. Rev. A **14**, 30 (1976).
[15]M. Gailitis and R. Damburg, Proc. Phys. Soc. London **82**, 192 (1963).
[16]P. L. Altick, Phys. Rev. A **38**, 5944(E) (1988).
[17]P. L. Altick (private communication).
[18]C. H. Greene, J. Phys. B **13**, L3 (1980).
[19]A. Pathak, A. E. Kingston, and K. A. Berrington, J. Phys. B **21**, 2939 (1988), and references therein.